Available online at www.eccomasproceedia.org
Eccomas Proceedia SMART (2023) 978-989

ECCOMAS
Proceedia

X ECCOMAS Thematic Conference on Smart Structures and Materials
SMART 2023
D.A. Saravanos, A. Benjeddou, N. Chrysochoidis and T. Theodosiou (Eds)

GUIDED WAVE BASED DAMAGE IDENTIFICATION IN COMPOSITE STRIPS USING INVERSE MULTIRESOLUTION WAVELET METHODS

DIMITRIS K. DIMITRIOU* **AND DIMITRIS A. SARAVANOS†**

* Department of Mechanical Engineering & Aeronautics
University of Patras
Rio-Patras, GR-26504, Greece
e-mail: d.dimitriou@upnet.gr

† Department of Mechanical Engineering & Aeronautics
University of Patras
Rio-Patras, GR-26504, Greece
email: dsaravanos@upatras.gr

Abstract. An inverse procedure for damage identification based on guided waves using the multiresolution finite wavelet domain method is presented. The forenamed method utilizes Daubechies wavelet and scaling functions for the approximation of state variables and as such, it involves two types of solutions, the coarse and the fine solutions. In that way, the multiresolution nature of the method can be utilized for efficient damage estimation in experimental applications since the fine solutions of the method have manifested remarkable localization capabilities and high sensitivity to damage. In order to fully take advantage of the additional functionalities of the multiresolution method, full-field displacement measurements of the guided wave propagation phenomenon are employed. Wavelet decomposition using Daubechies wavelets is now applied on the measurements in each different time step. The decomposition will lead to an approximation and a detail component that are directly comparable to the coarse and fine solution of the multiresolution simulation, respectively. Therefore, several multiresolution models can be created using the same Daubechies wavelets as the decomposition of the experimental data, so as to compare the simulation results with the measured ones. Numerical results evince that comparing the detail component of the experiments with the fine solution of the simulations, and their respective wavenumber spectra, using appropriate metrics can lead to efficient damage identification. In such manner, an optimization process can be conducted, utilizing the cross-correlation of both the structural responses and their wavenumber content for the definition of the objective function, in order to characterize the investigated damaged composite strip cases. This procedure can lead to more sensitive and accurate damage estimation due to the advantages of the multiresolution analysis.

Key words: Inverse methods, Guided waves, Damage detection, SHM, Multiresolution analysis, Composite structures.

Peer-review under responsibility of the organizing committee of SMART 2023.
doi: 10.7712/150123.9849.448984

1 INTRODUCTION

With the passage of time and the ever-increasing needs in fields such as the aerospace, naval, railway, public infrastructure industry, etc., the involved structural components become more complex. In order to objectively assess the state of those structural components, a procedure known as Structural Health Monitoring (SHM) involves collecting and analyzing data from a system of sensors that measure several quantities of the structural response. An SHM system's overarching goal is to be able to recognize instances of damage that may ultimately result in failure of the specific component or system at an early stage. The conclusions about the damage identified by monitoring may then be used to guide choices on corrective activities [1]. The SHM methods are divided into two main categories: the model-based and the data-based approaches. Model-based methods use inverse techniques in conjunction with physics-based models to update a set of parameters [2], [3] that lead to system identification or damage estimation. On the contrary, data-driven approaches use black-box methods such as machine learning techniques to obtain correlations between observed response data and structural degradation states [4], [5]. The guided wave-based SHM techniques is a major category of SHM methodologies that are widely studied due to the relatively cheap operational cost, the capability to scan large areas and the ability to detect small imperfections/damage [6], [7]. Many algorithms such as the delay-and-sum (DAS) [8], [9] and the time reversal [10], [11] and multiple signal classification (MUSIC) [12], [13] algorithms have also been extensively analyzed for damage imaging using guided waves.

In this work, the enhanced capabilities of the multiresolution finite wavelet domain method (MR-FWD) are investigated in the development of an inverse methodology using model update in order to provide damage estimation using guided wave propagation in composite strips. The MR-FWD method utilizes both the scaling and wavelet functions of the Daubechies wavelet family as basis functions, forming a hierarchical approach that involves two types of solution components: the coarse and the fine components. The method has evinced remarkable computational benefits in transient dynamic simulations of rods [14], Timoshenko beams [15] and high-order layerwise strips [16]. On top of the computation efficiency of the method, additional benefits have been manifested due to the sensitivity and localization properties of the utilized Daubechies wavelets [17]. The Daubechies scaling and wavelet functions act as a filter bank, with the scaling function performing as a low-pass filter and the wavelet function as a band-pass one. In that way, the coarse and the fine solution can approximate different structural responses based on the generated wavenumbers, and as such, the method provides extra damage detection capabilities. In the present paper, the multiple resolution components of the MR-FWD method are exploited for the model update process, in order to take advantage of the higher sensitivity of the fine solutions. To accomplish that, full-field measurements of the guided wave tests are considered to be available. Then the measurements are decomposed following the multiresolution decomposition [18] so as to obtain the approximation and detail component of the measurements that are comparable to the coarse and fine solution of the MR-FWD method, respectively. The case study that is presented in this paper manifests the great potential of the proposed inverse methodology and the higher sensitivity in the estimation of the damage parameters.

2 MR-FWD METHOD

The one-dimensional MR reconstruction and decomposition can be visualized in **Figure 1**.

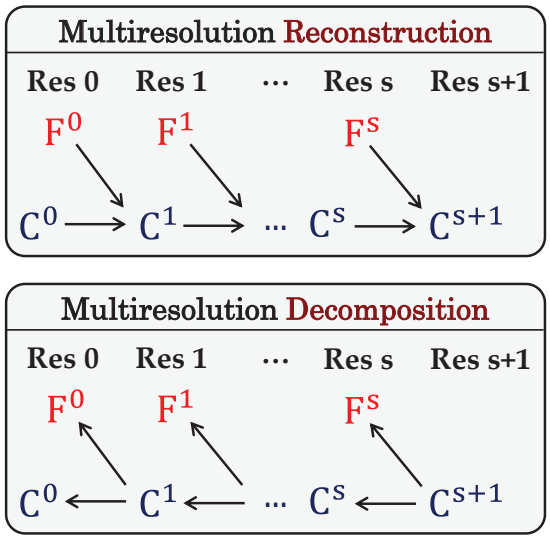

Figure 1: Schematic diagram of the 1D MR reconstruction and decomposition procedure.

Following the MR-FWD method, the 1D generalized displacement approximation for R resolutions is expressed by the following equation:

$$u(x,t) = \sum_{n=-(2L-2)}^{0} \hat{u}_{Cn}^{0}(t)\varphi(\xi - n) + \sum_{n=-(2L-2)}^{0} \{\sum_{S=0}^{R} \hat{u}_{Fn}^{S}(t)\psi(2^{s}\xi - n)\} \tag{1}$$

where $\hat{u}_{Cn}^{0}$ are the coarse wavelet coefficients at resolution 0, $\hat{u}_{Fn}^{S}$ are the fine wavelet coefficients at resolution S. Also, φ is the Daubechies scaling function (SF) and ψ is the Daubechies wavelet function (WF). A normalized local coordinate system ξ, is associated with each element. The MR procedure starts with the coarse solution (C^0), and then that solution is incrementally enriched by the fine solutions of each resolution (F^i).

Single-Resolution or Resolution 0 (C^0). The C^0 solution is obtained employing only the DB SFs and is the same as the FWD method. The equation of motion is:

$$[M_{CC}]\ddot{\hat{u}}_{CC}(t) + [K_{CC}]\hat{u}_{CC}(t) = F_C(t) \tag{2}$$

where $\hat{u}_{CC}$ are the generalized wavelet coefficients that correspond to the degrees of freedom of the coarse approximation, $[K_{CC}]$ and $[M_{CC}]$ are the coarse resolution stiffness and mass matrices, and F_C is the coarse resolution load vector.

Resolution 1 (C^1). According to the MR process, the fine solution at resolution 0 (F^0) needs to be calculated and added to the coarse solution at resolution 0 (C^0) so as to obtain C^1 solution. The MR solution system is:

$$\begin{bmatrix} M_{CC} & 0 \\ 0 & M_{FF} \end{bmatrix} \begin{Bmatrix} \ddot{\hat{u}}_C(t) \\ \ddot{\hat{u}}_F(t) \end{Bmatrix} + \begin{bmatrix} K_{CC} & K_{CF} \\ K_{FC} & K_{FF} \end{bmatrix} \begin{Bmatrix} \hat{u}_C(t) \\ \hat{u}_F(t) \end{Bmatrix} = \begin{Bmatrix} F_C(t) \\ F_F(t) \end{Bmatrix} \tag{3}$$

where $\hat{u}_F$ are the generalized fine wavelet coefficients, $\hat{u}_C$ are the generalized coarse wavelet coefficients for resolution 1, $[K_{FF}]$ and $[M_{FF}]$ are the fine resolution stiffness and mass matrices, respectively, and F_F is the fine resolution load vector. It should be highlighted that $\hat{u}_C$ is not equal to $\hat{u}_{CC}$ because of the stiffness coupling terms, $[K_{CF}]$ and $[K_{FC}]$. However, $[M_{CF}]$ and $[M_{FC}]$ are equal to zero because of the cross-orthogonality between SFs and WFs. Also, due to the orthogonality of SFs/ WFs, $[M_{CC}]$ and $[M_{FF}]$ are diagonal. More details about the MR-FWD method and the explicit integration of the multiresolution equations of motion can be found in [14]–[16].

3 INVERSE DAMAGE ESTIMATION PROCEDURE

The proposed inverse damage estimation methodology utilizes the multiple resolution components of the MR-FWD method so as to leverage the high sensitivity of its fine solutions. In order to do this, the experimental data should also be decomposed using the same SF, WF and resolution, to acquire the approximation and detail components of the data that are directly comparable to the coarse and fine solution of the MR simulation, respectively. The methodology, the utilized objective functions, the optimization process and the numerical results of the presented case study are shown in this section.

3.1 Methodology

The suggested methodology requires full-field data of the guided wave experiments. Those data are decomposed for each time step using a particular Daubechies SF/WF, i.e., the DB6, for a particular resolution level, i.e., one resolution level. In that way, two datasets are obtained, the approximation and the detail component of the experimental data. It should be highlighted that the detail component can provide additional information about the unknown parameters that we want to estimate, as shown in subsection 3.3. In that point, an optimization process can be performed using the MR-FWD method for the simulations in order to leverage the coarse and fine solutions that are directly comparable to the approximation and detail components. By utilizing appropriate objective functions, the design variables can be found and as such, the damage can be estimated. The whole inverse damage estimation approach is visualized in **Figure 2**.

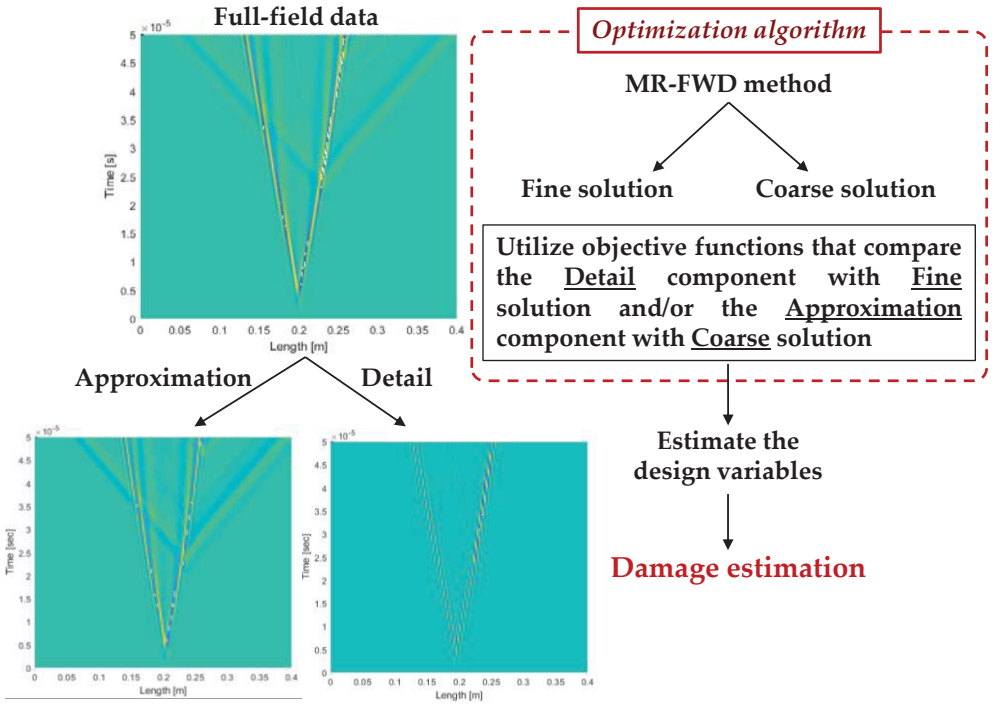

Figure 2: Damage estimation process using the MR-FWD method.

3.2 Objective functions

In the present paper, the objective functions include only the fine solutions of the MR-FWD simulations and the detail components of the pseudo-experimental data in order to manifest the higher sensitivity of the fine solutions. Two objective functions are simultaneously used for the optimization algorithm; the first compares the response of the fine solution with the detail component of the pseudo-experimental data in each time step, and the second compares their wavenumber spectra in a single timestep, namely, the last one.

More specifically, the first objective function compares the envelopes of the fine and detail component in each time step and then takes the average of those values. The envelopes are obtained using the absolute values of the Hilbert transforms of the detail and fine components. The utilization of the envelopes is crucial since a very small phase difference in the wave packets can erroneously result in large differences between two signals if the signals are directly compared. The first objective function is expressed as:

$$Obj1 = \sum_{t=1}^{T} \frac{\left\{\left|\mathscr{H}(fine(t))\right| * \left|\mathscr{H}(detail(t))\right|\right\}\{\tau = 0\}}{T} \tag{4}$$

where T are the total time steps, $\mathscr{H}(\cdot)$ is the Hilbert transform, $|\cdot|$ denotes the absolute value (or magnitude) of a complex number and $\{f * g\}\{\tau\}$ is the cross-correlation of f and g with lag τ. In that way, the comparison of the fine solution and detail component is performed

through the cross-correlation with zero lag. An investigation has been previously conducted in order to find the best comparison metric. The mean square error, cross-correlation, Wasserstein distance (WD) and dynamic time wrapping (DTW) were compared and the cross-correlation was found to be the most appropriate. The second objective function is given as:

$$Obj2 = \left\{ \mathcal{F}\left|(fine(t))\right| * \left|\mathcal{F}(detail(t))\right| \right\} \{\tau = 0\} \tag{5}$$

where t is the particular time step that the comparison of the wavenumbers takes place and $\mathcal{F}(\cdot)$ is the Fourier transform. Since the cross-correlation is a similarity metric, both objectives have higher values when the simulation is approaching the measured data. Considering that, the utilized optimization algorithm will try to find the maximum value of both objective functions, that can be utilized with same or different weights composing the final objective function. It is important to highlight that the information that gets lost from *Obj1* by performing the Hilbert transform to take the envelope of the response is retrieved by *Obj2* that compares the wavenumber content of the signals. Of course, the same objective functions could be employed for the comparisons of the coarse solution with the approximation component.

3.3 Case study

In this work, no experimental results are available due to the lack of full-field measurement apparatus. So, the "experimental" data are obtained from simulations in order to show the potential of the proposed methodology. The studied case refers to a damaged composite strip, with geometric characteristics that are shown in **Figure 3**.

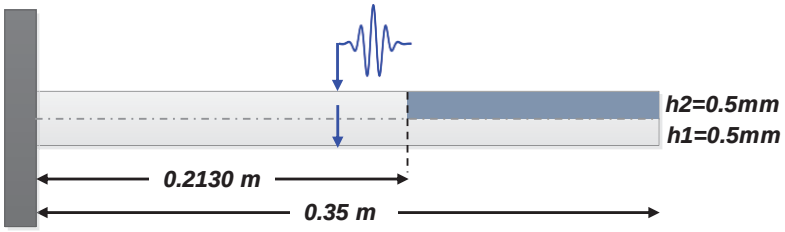

Figure 3: Schematic representation of the damaged composite strip, with the damage shown in dark gray color.

A 0.35 m long unidirectional damaged carbon/epoxy beam with 1 mm thickness and 20 mm width, clamped at its left edge and transversely excited at its center by a 5-cycle Hann windowed sine pulse with 200 kHz central frequency is modeled. The analysis duration is 0.05 ms. The mechanical properties of the pristine carbon/epoxy plies are shown in Table 1. The damage, which is modeled as 40% induced degradation in the elastic constants of the pristine material, spans from $0.213m \leq x \leq 0.35m$ lengthwise, and from $0.5mm \leq h \leq 1mm$ thickness-wise. Two discrete layers are used in the layerwise model to efficiently model the damaged region.

Table 1: Material properties.

	E_{11}(GPa)	$E_{22} = E_{33}$ (GPa)	$G_{12}=G_{23}=G_{13}$ (GPa)	$\nu_{12}=\nu_{13}$	ν_{23}	ρ (kg/m^3)
Carbon /Epoxy	120	7.9	3.4	0.275	0.15	1578

A single-resolution FWD analysis is employed for the acquisition of the "experimental" data, using 460 DB6 elements. A FE simulation could also have been used for the same purpose without any practical difference. The transverse displacement at the beam's top surface, termed as w^2 hereafter, is the quantity that is considered as measured by a full-field scanning vibrometer. In **Figure 4** the transverse displacement w^2 is displayed for the whole beam in both space and time, showing the evolution of the wave propagation phenomenon. It should be noted that from this response, no damage indication is visible or apparent.

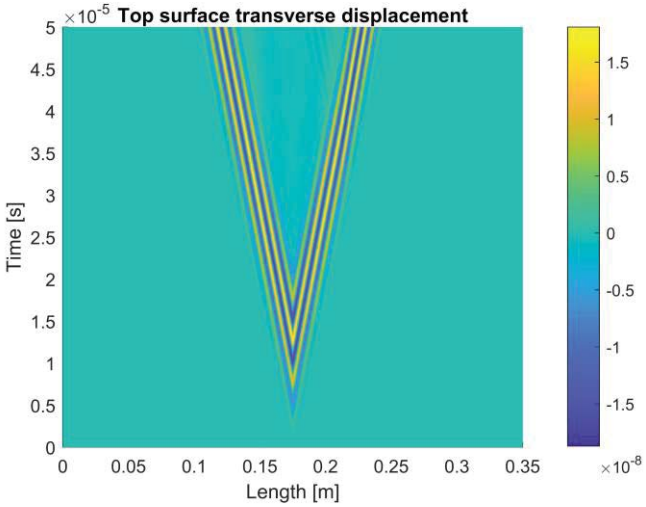

Figure 4: Transverse displacement field of top surface (w^2) of the damaged composite strip.

At this point, those data are decomposed in each time step using wavelet decomposition in one resolution with the Daubechies DB6 wavelet. Therefore, after this decomposition, an approximation and a detail dataset have emerged, as shown in **Figure 5**.

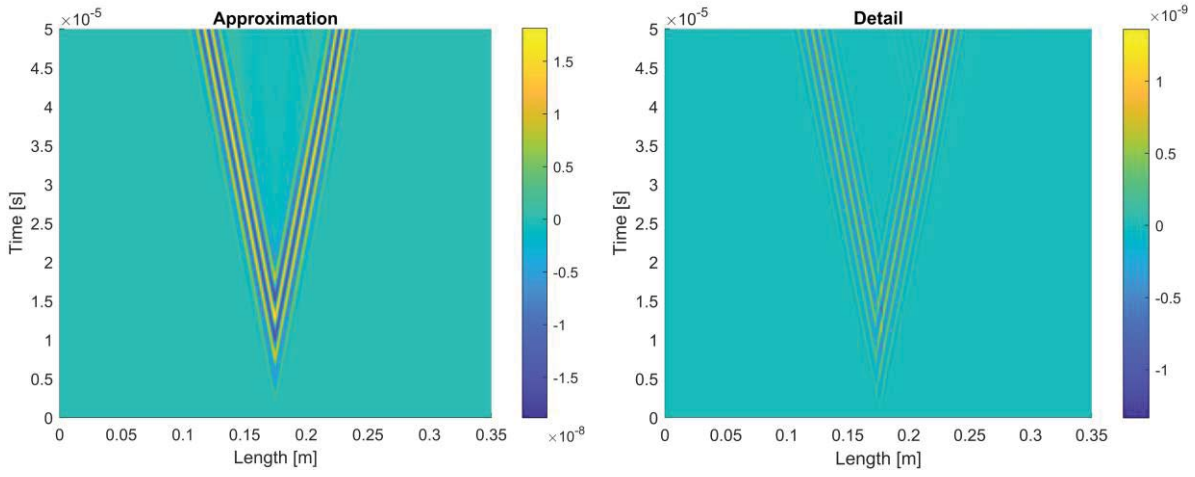

Figure 5: Approximation (left) and Detail (right) component of the w^2 displacement of the damaged composite strip after the wavelet decomposition.

It is obvious and expected that the approximation component is basically the same as the initial signal, namely, the w^2 displacement field. On the contrary, the detail component seems to have a different behavior, since it has much smaller amplitudes and the higher ones are focused on a specific range of the beam's length. This is sensible due to the localization properties of the wavelet functions that act as band-pass filters and lead to the determination of the detail component. In **Figure 6**, the normalized detail component is shown in a particular viewpoint in order to notice the reported higher values that provide additional localization information.

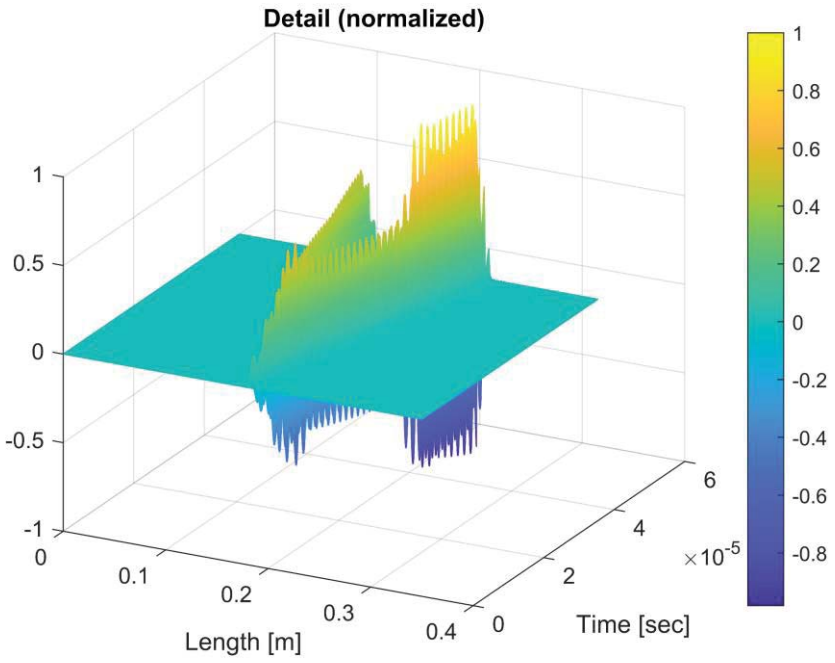

Figure 6: Detail component (normalized) of the displacement w^2 of the damaged composite strip.

The demonstrated localization functionality can lead to the estimation of the damage span, since it is apparent that the detail values become much larger after approximately $x=0.21m$. In that way, in the simulations that will be performed for the inverse damage detection process, that damage span can be considered known and so, the design variables can be fewer. Obviously, in many cases this will not be easily achievable or even feasible but, in any case, it is an additional advantage of the proposed methodology.

Moreover, the normalized fine solution of a MR-FWD model that corresponds to this case is presented in **Figure 7** in order to manifest the similarity of the decomposed detail component of the measured data with the fine solution of the MR-FWD analysis. In this analysis 230 DB6 elements have been utilized till resolution 1.

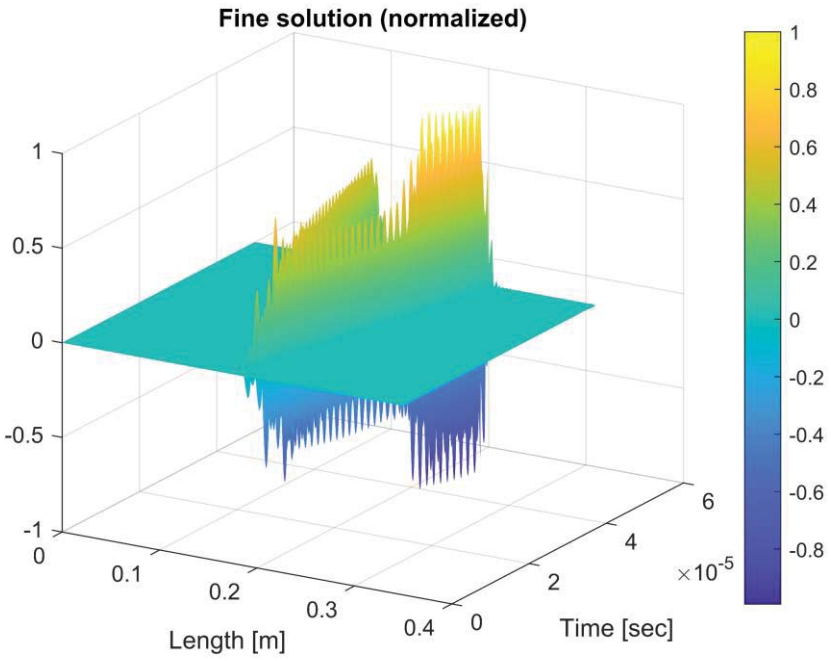

Figure 7: Fine solution (normalized) of the displacement w^2 of the damaged composite strip.

3.4 Optimization process & Results

Proceeding to the optimization process, the design variables should be established. In this case study, the design variables will essentially be the thickness ratio of the damaged span and the intensity of the damage. Specifically, the first design variable, termed as X1, is the coefficient which is multiplied with all the elastic constants to provide the damaged material. The second design variable, termed as X2, is the percentage of the height *h1*, that is shown in **Figure 3**, to the total height. The height *h2* is given by the subtraction between the total height and *h1*. The lower and upper bounds of the design variables are shown in Table 2.

Table 2: Design variables and their lower and upper bounds.

Design variables	Lower bound	Upper bound
X1	0.1	1
X2	0.1	0.9

The metaheuristic procedure that is employed in this work in order to solve the respective optimization problem is the Simulated Annealing (SA) algorithm [19], [20]. Several metaheuristic algorithms such as the Genetic algorithm [21] and the Particle Swarm Optimization [22] were tested before picking the SA algorithm due to its faster results using MATLAB® R2019b on a laptop with an Intel® Core i7-9750H @ 2.60 GHz CPU and 16 GB RAM. It should be highlighted that several runs have been performed with different initial values of the design variables due to the stochastic and single-solution nature of the SA

algorithm, but in any case, the algorithm resulted in the same final guesses. Furthermore, the same weights were used for the two objective functions (Eq. (4) and (5)) when forming the final objective function.

The results of the inverse methodology that is described in this paper are shown in Table 3. Two different approaches are performed and compared. The first one, called A1, is the one shown in **Figure 2** but using only the fine solution of the MR-FWD models and the detail component of the experimental signals in order to manifest the higher sensitivity of the fine solutions. The second approach, called A2, reminds the traditional model-based SHM approach where simulated results are directly compared to the experimental ones. In Table 3 the correct values and the values of the SA are presented when comparing either the fine solution of the MR-FWD model with the detail component of the experimental data or the total solution with the experimental data as is. Also, the percentage differences (PD) with the correct values are shown for each design variable. It should be noted that the termination criteria of the utilized SA algorithm were "loose" in order to obtain fast results, and that's why the estimated values show non-zero differences to the correct values.

Table 3: Results of the inverse damage estimation process and percentage differences (PD) of the estimated values to the correct ones.

	X1	X2	PD w.r.t. X1	PD w.r.t. X2
Correct values	0.6	0.5	0 %	0 %
A1: Fine solution vs. Detail component	0.5804	0.4988	3.2667 %	0.24 %
A2: Total solution vs. Experimental data	0.5765	0.5246	3.9167 %	4.92 %

It is obvious that both approaches have sufficient results, but the A1 approach is more sensitive and accurate than the A2 approach in both the design variables, and especially in the second one. This higher sensitivity and precision derive from the localization capabilities of the fine solution of the MR-FWD method and the detail components of the initial dataset that arises from the wavelet decomposition. It is worth to mention that the iterations of the SA algorithm of the A1 and A2 approach were approximately the same for the majority of the trials, but in some trials, the A1 approach required fewer iterations compared to the A2.

Moreover, if the same procedure was performed using any single-resolution method such as the FE, and then perform wavelet decomposition to the results in order to get the respective "coarse" and "fine" solutions, the following issues would rise:

i) those models are much slower than the MR-FWD simulations, as indicated in [15], [16].
ii) even if the accuracy was the same, the additional wavelet decomposition that is needed leads to a 5-13% slower process, depending on the utilized discretization, total degrees of freedom and number of iterations.

4 CONCLUSIONS

In this work, an inverse multiresolution method has been described for the damage detection of composite strips through model update. The proposed procedure leverages the multiple resolution components that the MR-FWD method provides in order to directly compare them with approximation and detail signals that arise from multiresolution decomposition of the

measured data. The presented numerical case study shows that this process can take advantage of the high sensitivity and localization properties of the fine solutions/detail signals, and so, it constitutes a precise damage identification approach based on updating specific design variables. Despite the relatively simple implementation of the described methodology in the present work, it seems a promising inverse procedure that deserves more extensive study and therefore, accounts for future research work.

ACKNOWLEDGMENTS

The research work was supported by the Hellenic Foundation for Research and Innovation (HFRI) under the 3rd Call for HFRI PhD Fellowships (Fellowship Number: 5509).

REFERENCES

[1] K. Worden, C. R. Farrar, G. Manson, and G. Park, "The fundamental axioms of structural health monitoring," *Proc. R. Soc. A Math. Phys. Eng. Sci.*, vol. 463, no. 2082, pp. 1639–1664, 2007, doi: 10.1098/rspa.2007.1834.

[2] D. Giagopoulos, A. Arailopoulos, V. Dertimanis, C. Papadimitriou, E. Chatzi, and K. Grompanopoulos, "Structural health monitoring and fatigue damage estimation using vibration measurements and finite element model updating," *Struct. Heal. Monit.*, vol. 18, no. 4, pp. 1189–1206, 2019, doi: 10.1177/1475921718790188.

[3] G. F. Gomes, F. A. de Almeida, A. C. Ancelotti, and S. S. da Cunha, "Inverse structural damage identification problem in CFRP laminated plates using SFO algorithm based on strain fields," *Eng. Comput.*, vol. 37, no. 4, pp. 3771–3791, 2021, doi: 10.1007/s00366-020-01027-6.

[4] A. Sattarifar and T. Nestorović, "Emergence of Machine Learning Techniques in Ultrasonic Guided Wave-based Structural Health Monitoring: A Narrative Review," *Int. J. Progn. Heal. Manag.*, vol. 13, no. 1, pp. 1–29, 2022, doi: 10.36001/ijphm.2022.v13i1.3107.

[5] A. Malekloo, E. Ozer, M. AlHamaydeh, and M. Girolami, *Machine learning and structural health monitoring overview with emerging technology and high-dimensional data source highlights*, vol. 0, no. 0. 2021.

[6] M. Mitra and S. Gopalakrishnan, "Guided wave based structural health monitoring: A review," *Smart Mater. Struct.*, vol. 25, no. 5, 2016, doi: 10.1088/0964-1726/25/5/053001.

[7] W. Ostachowicz, P. Kudela, M. Krawczuk, and A. Zak, *Guided Waves in Structures for SHM*. 2012.

[8] Z. Sharif-Khodaei and M. H. Aliabadi, "Assessment of delay-and-sum algorithms for damage detection in aluminium and composite plates," *Smart Mater. Struct.*, vol. 23, no. 7, 2014, doi: 10.1088/0964-1726/23/7/075007.

[9] M. M. Malatesta, R. Neubeck, J. Moll, K. Tschoke, and L. De Marchi, "Double-Stage DMAS With Fresnel Zone Filtering in Guided Waves Damage Imaging," *IEEE Trans.*

Ultrason. Ferroelectr. Freq. Control, vol. 69, no. 5, pp. 1751–1762, 2022, doi: 10.1109/TUFFC.2022.3162323.

[10] C. H. Wang, J. T. Rose, and F. K. Chang, "A synthetic time-reversal imaging method for structural health monitoring," *Smart Mater. Struct.*, vol. 13, no. 2, pp. 415–423, 2004, doi: 10.1088/0964-1726/13/2/020.

[11] J. K. Agrahari and S. Kapuria, "A refined Lamb wave time-reversal method with enhanced sensitivity for damage detection in isotropic plates," *J. Intell. Mater. Syst. Struct.*, vol. 27, no. 10, pp. 1283–1305, 2016, doi: 10.1177/1045389X15590269.

[12] C. Xu, J. Wang, S. Yin, and M. Deng, "A focusing MUSIC algorithm for baseline-free Lamb wave damage localization," *Mech. Syst. Signal Process.*, vol. 164, no. April 2021, p. 108242, 2022, doi: 10.1016/j.ymssp.2021.108242.

[13] Y. Lang, Z. Yang, D. Kong, W. Zhang, and X. Chen, "Forward-propagation-free focusing MUSIC algorithm for Lamb waves," *Struct. Heal. Monit.*, no. 28, 2023, doi: 10.1177/14759217231159868.

[14] C. V. Nastos and D. A. Saravanos, "Multiresolution Daubechies finite wavelet domain method for transient dynamic wave analysis in elastic solids," *Int. J. Numer. Methods Eng.*, vol. 122, no. 23, pp. 7078–7100, 2021, doi: 10.1002/nme.6822.

[15] D. K. Dimitriou, C. V Nastos, and D. A. Saravanos, "Multiresolution finite wavelet domain method for efficient modeling of guided waves in composite beams," *Wave Motion*, vol. 112, p. 102958, 2022, doi: 10.1016/j.wavemoti.2022.102958.

[16] D. K. Dimitriou, C. V Nastos, and D. A. Saravanos, "A multiresolution layerwise method with intrinsic damage detection capabilities for the simulation of guided waves in composite strips," *J. Vib. Control*, Mar. 2023, doi: 10.1177/10775463231158667.

[17] I. Daubechies, *Ten Lectures on Wavelets*. SIAM, 1992.

[18] S. G. Mallat, "A theory for multiresolution signal decomposition: The wavelet representation," *IEEE Trans. Pattern Anal. Mach. Intell.*, no. 7, pp. 494–513, 1989, doi: 10.1515/9781400827268.494.

[19] S. Kirkpatrick, C. D. Gelatt, and M. P. Vecchi, "Optimization by Simulated Annealing," *Science (80-.).*, vol. 220, no. 4598, pp. 671–680, May 1983, doi: 10.1126/science.220.4598.671.

[20] E. H. L. A. Peter J. M. Laarhoven, *Simulated Annealing: Theory and Applications*. Springer Dordrecht, 1987.

[21] J. H. Holland, *Adaptation in Natural and Artificial Systems: An Introductory Analysis with Applications to Biology, Control and Artificial Intelligence*. Cambridge, MA, USA: MIT Press, 1992.

[22] J. Kennedy and R. Eberhart, "Particle swarm optimization," in *Proceedings of ICNN'95 - International Conference on Neural Networks*, 1995, vol. 4, pp. 1942–1948 vol.4, doi: 10.1109/ICNN.1995.488968.